Chalcogenide Letters Vol. 16, No. 2, February 2019, p. 79 - 87

INFLUENCE OF RAPID THERMAL ANNEALING IN ARGON ATMOSPHERE ON PROPERTIES OF ELECTRODEPOSITED $CuInSe_2$ THIN FILMS: STRUCTURAL AND OPTICAL STADY

F. Z. SOUICI[a,b], B. BENHAOUA[a,c,*], H. SAÏDI[d], M. F. BOUJMIL[d], A. RAHAL[a,c], A. BENHAOUA[a,c], M. S. AIDA[e]

[a]*Lab. VTRS, Faculty of Science &Technology, University of El oued, El oued 39000, Algeria*

[b]*Faculty of Mathematics and Material Sciences, Univ. Ouargla, Ouargla 30000, Algeria*

[c]*Unité de developpement des Energies Renouvelables dansles Zones Arides (UDERZA), University of El oued, El oued 39000, Algeria*

[d]*Photovoltaic Laboratory, Center for Research and Technology of Energy, Technopole of Borj-Cédria, BP.95, 2050 Hammam-Lif Tunisia*

[e]*Faculty of Science King Abdulaziz University Jeddah Saudi Arabia*

In this article, electrochemically as deposited and rapid thermal annealing in argon atmosphere of $CuInSe_2$ thin films were investigated. The annealing treatments, for half an hour in argon atmosphere, were done at 250°C, 300°C and 350°C. Structural and grain sizes, morphological surfaces and optical properties, of the as deposited and annealed $CuInSe_2$ thin films of different heat treatments were compared. All elaborated thin films show the tetragonal chalcopyrite $CuInSe_2$ with favored orientation along (*112*) direction. Grain seizes of the as deposited film was about 24.48 nm whereas the annealed thin film at 350°C presents the high intensity of (*112*)peak with high grain size of 40.71nm. To support XRD and SEM results relating to the composition and quality of the as deposited and annealed $CuInSe_2$ thin films, FT-IR spectroscopy investigation was used. It reveals a distinct absorption peaks nearly at 2332-2361cm^{-1} conforming the $CuInSe_2$ product. The band gap of the samples was found to be in 1.10-1.20eV range. As a result, RTP conditions of the films are found to be of interest in the process of $CuInSe_2$ electro-deposition and its crystallinety enhancement. As active absorber layers for solar cell applications, those thin films may be used.

(Received November 20, 2018; Accepted February 11, 2019)

Keywords: Thin films, $CuInSe_2$, Electro-deposition, Rapid thermal annealing, X-ray diffraction

1. Introduction

Copper indium diselenide ($CuInSe_2$ or CIS) is a 1.02eV direct band gap material with high optical absorption coefficient (10^{+5} cm^{-1}) [1-3], good stability and high efficiency [4,5] these factors make it as promising absorber material for thin film solar cells. As well-known, there are multiple techniques currently available for the preparation of CIS thin films, for instance co-evaporation [6], RF sputtering [7], molecular beam epitaxial[8], spray pyrolysis [9], pulsed laser deposition[10], and electro-deposition[11]. The later has various advantages such as (i) low cost, (ii) large scale area of deposition, (iii) high speed deposition (iv) vacuum system less, and (v) no use of toxic gases [12].

As recognized, the electrical, optical, morphological and structural properties of such elaborated material are really influenced by the techniques and the experimental parameters. In electro-deposition method, the precursor concentration, complexing agent[13], potential, time deposition and post annealing treatment are the common parameters that influence the material

*Corresponding author: benhaouab@yahoo.fr

properties. Post annealing treatment is required to improve the crystallinity of CIS thin films. But based on the low vapor pressure of Selenium, thin films annealed in vacuum, nitrogen or argon atmospheres usually present high levels of Se vacancies [14-16]. For this reason, selenization (ie: excess of selenium as H_2Se gas in the surrounding atmosphere of annealing) may be obligatory to compensate selenium loss and adjust the stoichiometry of $CuInSe_2$ thin films. Although, the elevated toxicity of selenium gas, which can be considered as an edge for mass production of CIS-devices [17], re-crystallization was carried out at 550°C in the selenium atmosphere as a solution to prevent selenium less in the thin film [18]. Recent studies using wet chemical without annealing to avoid desalination, CIS nanoparticles are synthesized[19]

It is worth noting that the effects of classical annealing, on CIS physical properties, are widely studied, but more investigations namely on the mode and the atmosphere of annealing are still required.

This work aims to electrochemically deposit CIS thin films and to study the effect of rapid thermal annealing in argon atmosphere (RTAAA), on their properties and to compare them to the as deposited one. On coated indium tin oxide substrate (ITO), those CIS thin films are deposited. To characterize the structural, surface morphology and optical properties, X-ray diffraction (XRD), scanning electron microscopy (SEM), UV-visible near infrared transmission and FT-IR spectroscopy techniques are used, respectively.

2. Experimental

The electrodeposition of CuInSe2 (CIS) thin films were performed using an a potentiostat model Voltalab 40 with a three-electrode cell, which consists of a platinum plate as the counter electrode, a saturate calomel (Ag/AgCl) as the reference electrode and an ITO coated glass as the working electrode on which CIS thin films were deposited for 15min. For the RTP in (AA), an infrared furnace was used to anneal the deposited films. The furnace consists of lighting infra-red lamps around a quartz tube. The lamps were powered by an electrical regulating source and the annealing temperature was stepped as 250°C, 300°C and 350°C for maintained time of 30 min. Prior to deposit on ITO glass, the later was cleaned ultrasonically with acetone, and ethanol during 10 min for each treatment; then the cleaned glass was rinsed with distilled water and blow-dried in the air. CIS thin films were electrochemically deposited from a solution of $CuCl_2$, $InCl_3$ and SeO_2 at given concentration (3.5, 3.5 and 7mM), respectively. The added complexing agent was Na-citrate at 0.5 M whereas the pH was taken closely 1.5 [20]. The bath was adjusted to this pH by adding diluted hydrochloric acid. At room temperature, each film deposition was proceeded for 15 min (t=15min).The potential deposition was maintained constant at (-950mV/SCE), without stirring[21].

For the RTP in (AA), some of the as deposited films were held in quartz tube. The RTAAA consists of lighting infra-red lamps around the quartz tube. The lamps were powered by an electrical regulating source. While the annealing temperatures were 250°C, 300°C and 350°C for 30 min. The as deposited and treated samples constituting the samples for this study are named (a), (b), (c) and (d), respectively. Structural properties were carried out using XPERT-PRO X-ray diffractometer with CuK_α radiation in the scanning angle range of 10-80° whereas morphological properties of the samples surfaces were survived by means of SEM apparatus. To hold up XRD and SEM results, the quality and composition of the films were investigated by FT-IR spectroscopy apparatus(Agilant Technologie carry 600 series FTIR). The scan of the FT-IR measurements investigation of the CIS bonding formation was performed in (400-4000cm^{-1}) range. For this purpose, only the as deposited and 300°C treated samples were taken in consideration. Transmittance and optical properties of the prepared films such as band gap (E_g) were studied using Shimadzu mode UV-3101 PC spectrophotometer. It was taken in consideration that the streak light of the apparatus confronts directly the CIS face.

The thickness (d) of the as elaborated thin films was theoretically estimated as follows[22]:

$$d = \frac{1}{nFA}\left(\frac{ItM}{\rho}\right) \quad (1)$$

where n is the number of transferring electrons, F is the Faraday's number, A is the electrode area, I is the applied current, t is the deposition time, M = 336.28 g/mol is the molecular weight, ρ = 5.77 g/cm^3 is the density and n is taken equal to 13 exchanged electrons.

$$Cu^{+2} + In^{+3} + 2SeO_3^{-2} + 12H^+ + 13e^- \rightarrow CuInSe_2 + 6H_2O \quad (2)$$

For all evaluated simples the thickness average was 1.10-1.19µm before annealing treatment which is still as estimation hence the film areis not well homogeneous.

3. Results and discussion

3. 1. Structural properties

For 15 min time deposition CIS thin films, X-ray diffraction patterns of the as deposited and annealed ones with the pattern of the ITO covered glass are given in Fig.1. If one starts by describing the bellow spectrum of ITO on which chalcopyrite CIS films were deposited. It exhibits six diffraction peaks located at 2θ = 21.497°, 30.858°, 35.462°, 45.688°, 51.024° and 60.667° which related to the following planes (*211*), (*222*), (*400*), (*431*), (*440*), and (*622*), respectively. Such peaks much well with those of the Joint Committee on Powder Diffraction Standards (JCPDS) card (No. 71-2195) of the cubic In_2O_3:Sn structure (ITO). Whereas X-ray diffraction patterns of the as deposited and annealed CIS thin films exhibit three major diffraction peaks at 2θ = 26.82°, 44.5°and 52.49 which are related to (*112*) plane and to the subsequent emerged (*204*)/(*220*) and (*116*)/(*312*) ones, respectively. All the diffraction peaks coordinated well with the space group I-42d (*122*) matching to the tetragonal chalcopyrite CIS phase having JCPDS card (No. 40-1487). Peak (*112*), located at 2θ°=26.82 is present in the whole spectrum which is the most intense peak given in the JCPDS file for the CIS phase. No peak of the binary compounds was observed however others residual diffraction peaks, with feeble intensities, located at 2θ = 21.497°, 30.858°,35.462°, and 51.024° subsist in the spectrum. Those residual diffraction peaks found their origin from the inner X-ray diffraction on ITO covered glass, on which the films were deposited. As it was seen in (Fig.1 samples b, c and d), with increasing annealing temperature from 250°C to 350°C, peak intensities of (*112*)plan, (*204*)/(*220*) and (*116*)/(*312*) emerged plans increase leading to an enhanced crystallinity of the sample treated at 350°C. Such peaks are established by many authors using the argon atmosphere treatment [23-26]. Within the XRD detection limit, for the treatment at 350°C three additional peaks corresponding also to chalcopyrite CIS phase [27,28], which are located at 2θ = 17.12°, 64.67° and 70.94° related to (*101*), (*400*) and (*316*) plans, respectively.

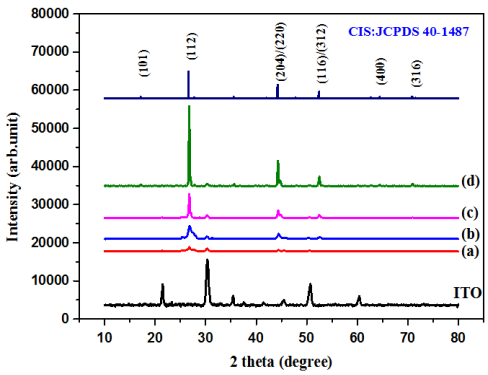

Fig. 1: XRD patterns of ITO coated glass substrate with as deposited and 30min annealed CIS thin film, in argon atmosphere: a) as deposited, b), c) and d) annealed at 250, 300 and 350°C respectively.

For more details, about the preferred growth orientation, different texture coefficients *TC(hkl)*, representing the texture of the particular plane, were determined using the X-ray data. *TC(hkl)* coefficients were calculated via the well-known formula [29].

$$TC(hkl) = \frac{I(hkl)/I_0(hkl)}{N^{-1}\sum_n^N I(hkl)/I_0(hkl)} \quad (3)$$

where *I(hkl)* is the measured relative intensity of a plane *(hkl)*, I_o*(hkl)* is the standard intensity of considered plane taken from the JCPDS data, *n* is the number of diffraction peaks and *N* is the reflection number.*TC(hkl)* values of all films for (*112*), (*204*)/(*220*) and the emerged (*116*)/(*312*)peaks, with the annealing temperatures are shown in Fig. 2. The polycrystallinity nature of the films was confirmed since the values of *TC(hkl)* are lower than unity. Observing this figure one can see that the whole thin films have privileged orientation along the (*112*) plan and the crystalline quality of thin films improved with 350°C as annealing temperature.

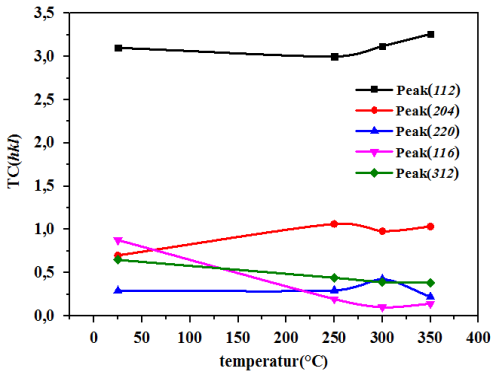

Fig. 2: Variation of TC (hkl) with annealing temperatures in argon atmosphere of CIS thin films.

The crystallite size of the as deposited and annealed CIS thin films was calculated from the high intensity of (*112*)direction peaks, obtained from the diffraction patterns, using the full width at half maximum (*FWHM*) and Scherrer's formula [30]:

$$D = \frac{0.9\lambda}{\beta \cos\theta} \quad (4)$$

where ***D***, ***β*** and ***λ*** are the crystalline size, *FWHM* of the most intense diffraction peak, and the X-ray wavelength (1.54056 Å) whereas ***θ*** is the Bragg angle of peaks (*112*) for the as deposited and annealed CIS thin films taken in consideration. Scherrer's equation applied to the most intense (*112*) peaks diffraction lines of those films, respectively. It reveals that ***D*** size distribution is about 24.48nm for the as deposited and increases with annealing temperature to reach 40.71nm as exhibited on Fig.3 and recapitulated in Table1.

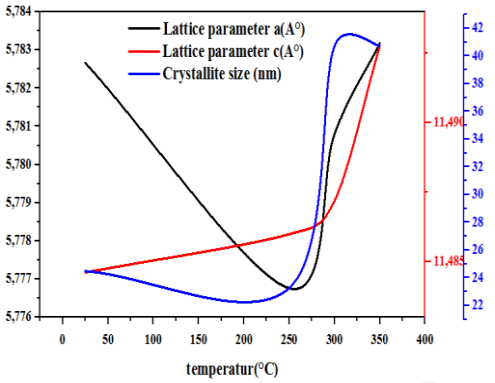

Fig. 3: Lattice parameters (a and c) and Crystallite size (D) of CIS thin films with annealing temperatures.

According to the tetragonal chalcopyrite CIS phase, the lattice constant can be calculated by the following formula:

$$\frac{1}{d_{hkl}^2} = \frac{h^2+k^2}{a^2} + \frac{l^2}{c^2} \quad (5)$$

where *a*, *c*, (*hkl*) and $\boldsymbol{d}_{hkl}$ are the lattice parameters, the Miller indices of the planes and its corresponding interplanar spacing. These parameters are shown in Table 1. In Fig. 3 it was reported the variations of the crystallite size and the lattice parameters *a* and *c*, of all CIS thin films. As can be seen from Fig. 3 and Table 1, the crystallite size was round 24.48nm for the as deposited. After annealing in argon atmosphere at 250°C, it remains approximately constant (23.26nm) then increases to reach 40.71nm as edge value when the samples were annealed at 300°C and at 350°C. This leads to proclaim that beyond 300°C a treatment limit effect happens. The values of the lattice parameters *a* and *c* have slight change with annealing treatment: *a* has a slight decrease with the annealing at 250°C, then increases with temperature, whereas *c* evokes an increasing with annealing temperature but it is still less than the standard parameter c_0 =11.6100Å obtained from the JCPDS card (No. 40-1487). The *c* week values lead to announce that the elaborated lattice is stressed along this direction.

Table 1: The lattice parameter (a and c) and d-spacing of (112) plan, Crystallite size (D) and band gap energy (E_g) of as deposited and 30min annealed CIS thin films.

Samples	Crystallite size(nm)	$d_{(112)}$ (Å)	E_g (eV)	Lattice constants (Å)			
				a	$\Delta a = a - a_0$	*c*	$\Delta c = c - c_0$
As deposited	24.48	3.33080	1.20	5.78266	–0.00066	11.48460	–0.1254
Annealed at 250°C	23.26	3.32867	1.16	5.77675	–0.00525	11.48598	–0.1240
Annealed at 300°C	40.71	3.33034	1.14	5.78079	–0.00121	11.48718	–0.1228
Annealed at 350°C	40.71	3.33179	1.10	5.78317	–0.00120	11.49276	–0.1172

3. 2. Morphological properties

At the equal magnification, Fig. 4 exhibits the SEM morphologies of all the CIS thin films prepared from fixed electrolyte concentration (3.5mM $CuCl_2$, 3.5mM of $InCl_3$, 7mM of SeO_2) for 15 min deposition. Starting by Fig. 4a, it represents the as deposited CIS thin film. As seen the surface contains a multinuclear, cauliflower-like and (desert rose-like) grains crystalline structure of CIS. Cauliflower and desert rose-like aggregation with rounded well-defined boundaries are found distinctively on the surface of the film. Such difference in the structure may be associated to the potential distribution on the surface during electro-deposition. Similar cauliflower-like morphology was observed by many authors [13,21,25,31-33]; whereas desert rose-like morphology was observed by Yassitepe et al [28] . The grains crystalline structure of CIS is well detected by XRD measurement. For the heated CIS thin films and in respect to the temperature rise, the sample annealed at low temperature 250°C, the boundaries of rounded granular structure diminish and inter diffuse to form homogenous CIS layer (see in Fig. 4b).With increase (RTAAA) temperature, the inter diffusion of rounded granular structure continues to enhance the CIS layer homogeneity with, of course, losing its big dimension as it was seen in Fig. 4c. Displayed in Fig. 4d is the film having the most homogeneous layer, than any others films with few residual little rounded granular grains. The homogeneous coalescence of the neighboring nodules is improved because of the elevation of (RTAAA) temperature to 350°C leading to enhanced crystalline structure. Such enhancement is well confirmed by XRD measurements.

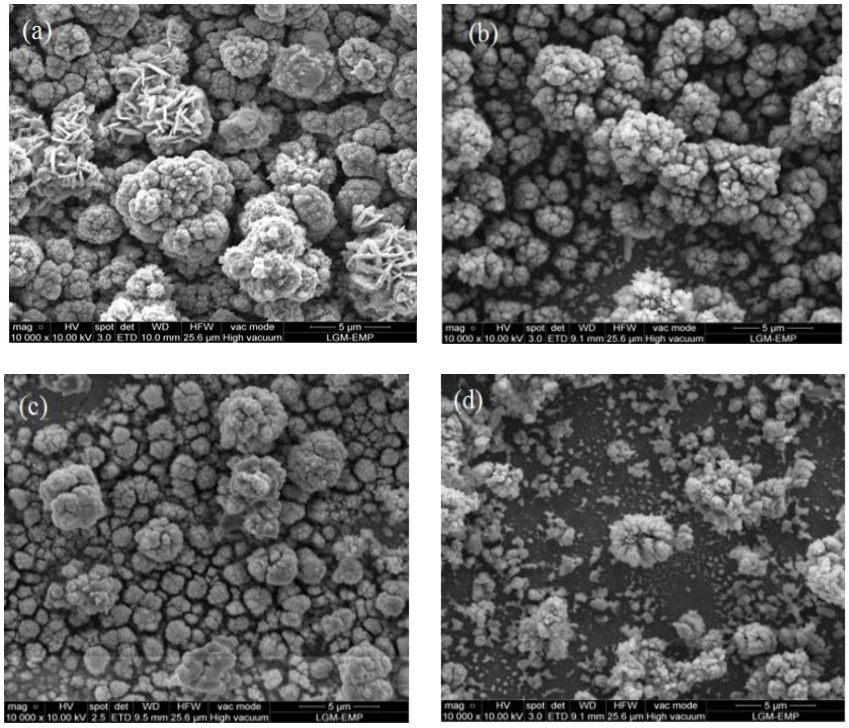

Fig. 4: SEM images of CIS thin films: a) as deposited, b), c) and d) 30min annealed in argon atmosphere at 250, 300 and 350°C, respectively.

3. 3. FT-IR analysis

To further support the XRD and SEM results, the quality and composition of CIS thin films were investigated by FT-IR spectroscopy which is known as one of the very practical method to find out information about matter chemical bonding and elemental constituents. Fig. 5 shows FT-IR spectra of as deposited and (RTAAA) at 300°C CIS thin films. For both samples, a dissimilar absorption peaks are observed nearly at 2332-2361cm^{-1} and another peaks at 1527cm^{-1} with less absorption corresponding to the CuInSe2stretching vibrations modes[26]. But for the annealed thin film at 300°C the absorption peaks intensities was found to be greater than before annealing which confirms the raise in amount of CuInSe2 bonding. This reveals the effect of the (RTAAA)in enhancing the thin films quality as it was carried out by XRD and SEM results. It may proclaimed that (RTAAA) acts as brake for the Se out diffusion and offers an adequate amount of Se to the CIS thin films to crystallize better than other use of classical thermal annealing.

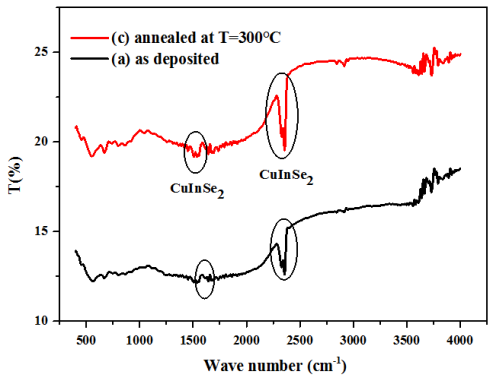

Fig. 5: FT-IR spectra of CIS thin films: a) as deposited sample b) annealed at 300°C in argon atmosphere.

3. 4. Optical properties

Fig. 6 gathers the transmittance patterns of as deposited and 30min annealed CIS thin films. As seen in Fig. 6a-d, the transmittance of the as deposited and annealed CIS thin films, at 250, 300 and 350°C, respectively, reveals a feeble transmittance values due to the whole absorbance of light by those layers mainly in the region between 400-1800nm. A strong absorbance was remarked with the film treated at 350°C (see Fig. 6d).

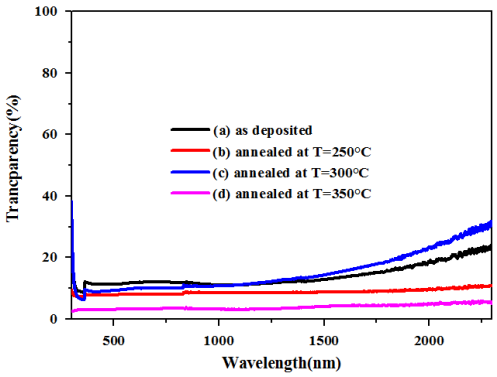

Fig. 6: Optical transmittance of as deposited and annealed CIS thin films in argon atmosphere: a) as deposited, b), c) and d) 30min annealed CIS thin films at 250, 300 and 350°C, respectively.

As it was known that CIS is a direct gap semiconductor, so the absorption coefficient (α) in the region of strong absorption obeying to the equation[34]:

$$(\alpha h\nu)^2 = B\left(h\nu - E_g\right) \tag{6}$$

where α is the absorption coefficient, h is the Planck constant, ν is the radiation frequency, E_g is the band gap energy and B is a constant which depends on the nature of the radiation. The band gap (E_g) values of as deposited and 30min annealed CIS samples were deduced from the transmittance data, in region 400-1800nm, according to Tauc's relation [35] giving $(\alpha h\nu)^2$ versus incident photon energy, ($h\nu$), plots. The graphs are represented in Fig. 7, whereas the band gap energy values are illustrated in Table 1. All the samples exhibit linear wavelength absorption dependence around the optical band gap which is characteristic of the direct inter-band transition. E_g values of the as deposited and annealed at 250, 300 and 350°C CIS thin films were found to be 1.20, 1.16, 1.14 and 1.10eV respectively. Such values were found out by several researchers. They are slight larger than one reported for the bulk $CuInSe_2$ of 1.05 eV[36] evoking a blue shift in E_g value. This shift may be owing to quantum confinement arising due to size effect[19].As can be seen from Table 1, a small decrease in E_g with the annealing temperature was remarked. This decrease is almost certainly due to the rearrangement of the atoms in the crystalline lattice, to the decrease of the defects in microstructure and to quantum detention of the treated thin films. As result, the annealed thin films may be used as an active absorber layers for solar cell applications.

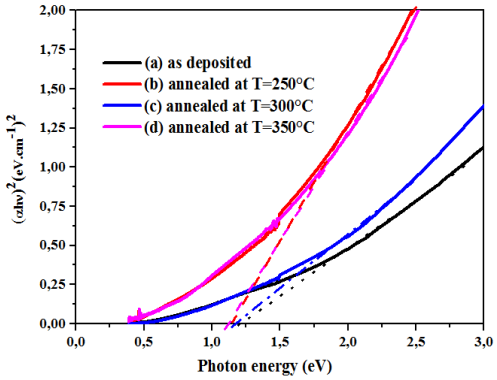

Fig. 7: Band-gap (E_g) estimation, from Tauc's relation, of as deposited and 30min annealed CIS thin films: a) as deposited, b), c) and d) annealing at 250, 300 and 350°C, respectively.

4. Conclusions

In this study, for 15min. effects of (RTAAA), for 30 min at 250°C, 300°C and 350°Celectrochemically deposited CIS thin films were investigated. XRD studies show that all the elaborated thin films have the tetragonal chalcopyrite CIS structure with favored orientation along (*112*) direction. The as deposited CIS sample has grain seize about 24.48nm. While the annealed one at 350°C has the high intensity of (*112*) plane with high grain size of 40.71nm and exhibits the better crystalline structure in this work. SEM images display cauliflower and desert rose-like aggregations located distinctively on the surface of the film and inter diffuse with the (RTAAA) temperature raise to form CIS layers.

FT-IR spectra of as deposited and annealed at 300°CCIS thin films confirm XRD and SEM results by showing an absorption peaks nearly at 2332-2361cm^{-1} corresponding to $CuInSe_2$ structure. The absorption peaks intensities were found to be greater after (RTAAA) confirming the raise in amount of CuInSe2 bonding. This proceeds by offering the films an adequate amount of Se to crystallize better than other use of classical thermal annealing. The optical properties of the films were greatly influenced by this method of treatment. Such treated thin films may be used as actives absorber layers for solar cells use.

Acknowledgments

This work was supported in part by CNEPRUE project code No: B00L02UN390120150001 and VTRS laboratory of El-Oued University. X-ray diffraction data in this work were acquired with an instrument supported by Technical Pole of Borj Cedria, Tunisia. We thank Mohamed Jlassi and Houda Saïdi for their assistance in XRD data acquisition and annealing of the samples.

References

[1]N.Kavcar, M.Carter, R.Hill, Solar Energy Materials and Solar Cells **27**, 13 (1992).
[2]R.Sharma, K.Sharma, J.Garg, Journal of Physics D: Applied Physics **24**, 2084 (1991).
[3] C. Rincón, Solid State Communications**64**, 15 (1987).
[4] S.Kundu, M.Basu, S.Chaudhuri, A.Pal, Thin Solid Films **339**, 44 (1999).
[5] B.Eisener, M.Wagner, D.Wolf, G.Müller, Journal of Crystal Growth**198**, 321 (1999).
[6] E.Don, R.Hill, G.Russell, Solar Cells **16**, 131 (1986).
[7] T.Yamaguchi, J.Matsufusa, H.Kabasawa, A. Yoshida, Journal of Applied Physics **69**, 7714 (1991).
[8]S.Niki,P. Fons, A.Yamada, T.Kurafuji,S. Chichibu, H.Nakanishi, W.Bi, C. Tu, Applied Physics Letters **69**, 647 (1996).
[9] C.R.Abernathy, C.W.Bates Jr, A.A.Anani, B.Haba, G.Smestad, Applied Physics Letters **45**, 890 (1984).
[10]S.Kuranouchi, A.Yosbida, Thin Solid Films **343**, 123 (1999).
[11]A.Molin, A.Dikusar,G. Kiosse, P.Petrenko, A.Sokolovsky,Y.G. Saltanovsky, Thin Solid Films **237**, 66 (1994).
[12] S.H.Kang, Y.-K.Kim, D.-S.Choi, Y.-E.Sung, Electrochimica Acta **51**, 4433 (2006).
[13]T.-J.Whang, M.-T.Hsieh, Y.-C.Kao, Applied Surface Science **257**, 1457 (2010).
[14] S.Sahu,R. Kristensen, D. Haneman, Solar Energy Materials **18**, 385 (1989).
[15] C.Huang, T.Meen, M.Lai, W.Chen, Solar Energy Materials and Solar Cells **82**, 553 (2004).
[16] M.Valdés, M.Frontini,M. Vázquez, A.Goossens, Applied Surface Science **254**, 303 (2007).
[17] M.Valdés, M. Vázquez, Electrochimica Acta **56**, 6866 (2011).
[18] J.Wellings, A.Samantilleke, S.Heavens, P.Warren, I.Dharmadasa, Solar Energy Materials and Solar Cells **93**, 1518 (2009).
[19] S.M.Chauhan, S.H.Chaki, M.Deshpande, J.P.Tailor, A.J.Khimani, A.V.Mangrola, Nano-Structures & Nano-Objects **16**, 200 (2018).

[20] J.Xu, X.Yao, J. Feng, Solar Energy Materials and Solar Cells **73**, 203 (2002).
[21] R.Yu, T.Ren, C.Li, Thin Solid Films **518**, 5515 (2010).
[22]F.-Y.Liu, L.Ying, Z.-A.Zhang,Y.-Q. Lai, L.Jie, Y.-X. Liu, Transactions of Nonferrous Metals Society of China **18**, 884 (2008).
[23] A.Palacios-Padrós, F.Caballero-Briones, F.Sanz, Electrochemistry Communications **12**, 1025 (2010).
[24] W.-T.Chiu, S.-W.Chen, S.-M.Tseng, Solar Energy Materials and Solar Cells **141**, 187 (2015).
[25] Y.-S.Chiu, M.-T.Hsieh, C.-M.Chang, C.-S.Chen, T.-J.Whang, Applied Surface Science, **299**, 52 (2014).
[26]A.-H.Kashyout, E.-Z.Ahmed, T.Meaz, M.Nabil, M. Amer, Alexandria Engineering Journal **53**, 731 (2014).
[27] J.-S.Hahn, G.Park, J.Lee, J. Shim, Journal of Industrial and Engineering Chemistry **21**, 754 (2015).
[28]E.Yassitepe, W.N.Shafarman, S.I.Shah, Journal of Solid State Chemistry **213**, 198 (2014).
[29]C.Barrett, T. Massalski, Structure of Metals Pergamon Press. Oxford: 1980.
[30] P.Scherrer, Nachr. Ges. Wiss. Göttingen **2**, 96 (1918).
[31] T.-J.Whang,M.-T. Hsieh, Y.-C.Kao, S.-J.Lee, Applied Surface Science **255**, 4600 (2009).
[32] K.De Silva,W. Priyantha, J.Jayanetti,B. Chithrani, W.Siripala, K.Blake, I.Dharmadasa, Thin Solid Films **382**, 158 (2001).
[33] M.Valdes,M. Vázquez, A. Goossens, Electrochimica Acta **54**, 524 (2008).
[34]R.Bube, A.Fahrenbruch, Fundamentals of solar cells. AcademicPress, London, New York, 425 (1983).
[35] J.Tauc, Amorphous and Liquid Semiconductors (Plenum Press, New York, 1974).
[36] J.Ebenezar, Recent Trends in Materials Science and Applications: Nanomaterials, Crystal Growth, Thin Films, Quantum Dots, & Spectroscopy (Proceedings ICRTMSA 2016); Springer: **189**(2017).